

# Magnetic fields and large-scale structure in a hot universe

## II. Magnetic flux tubes and filamentary structure

E. Florido and E. Battaner

Dpto. Física Teórica y del Cosmos, Universidad de Granada, Spain

Received 25 September 1996 / Accepted 8 April 1997

**Abstract.** In Paper I, we obtained an equation for the evolution of density inhomogeneities in a radiation dominated universe when they are affected by magnetic fields. In this second paper we apply this equation to the case in which the subjacent magnetic configuration is a flux tube. For scales of the order of 1 Mpc or less the differential equation is elliptical. To solve it, we have used the numerical method based on “Simultaneous Over Relaxation”, SOR, with Chebyshev acceleration and we have treated the problem as a boundary value problem, which restricts the prediction ability of the integration. For large-scale flux tubes, much larger than 1 Mpc, the equation can be analytically integrated and no assumption about the final shape or magnitude of the inhomogeneity is required. In both cases we obtain an evolution which does not differ very much from linear in time. The inhomogeneity in the density becomes filamentary. Large scale structures ( $\geq 10$  Mpc) are probably unaffected by damping, non-linear and amplification mechanisms after Equality, so that this model provides a tool to interpret the present observed large scale structure. Filaments are very frequently found in the large-scale structure in the Universe. It is suggested here that they could arise from primordial magnetic flux tubes, thus providing an alternative hypothesis for its interpretation; in particular we consider the case of the Coma-A1367 supercluster, where the magnetic field is known to be high.

**Key words:** magnetohydrodynamics – relativity – cosmology: large-scale structure of Universe

### 1. General equations

In Paper I, we presented the basic equations governing the evolution of the large scale energy density structure in the pre-recombination universe, when the effect of magnetic fields cannot be ignored. In the linear regime, the magnetic field configuration remains time-independent throughout this era, only growing with the expansion. The degree and the way this field structure affects the evolution of density inhomogeneities would depend on the

particular pattern of the magnetic field lines. We will consider here a small cell in which the magnetic field has the simplest structure: a magnetic flux tube. Different sizes of the flux tube will be considered, for small, intermediate and large scales.

We will deal with the integration of Eq. (86) of Paper I

$$\ddot{\delta} - \delta - X + \frac{1}{3}e^{-\tau}\nabla'^2\delta + 2e^{-\tau}m = 0$$

where:

$\delta$  is the relative energy density contrast, defined as  $\delta\epsilon/\epsilon$ , where  $\epsilon$  is the energy density and  $\delta\epsilon$  the difference between its value within the inhomogeneity and its mean value in the Universe. As we are considering relativistic particles, we also have  $\delta = \delta p/p$  where  $p$  is the hydrostatic pressure of the relativistic particles (either photons or any hot dark matter particles).

$\ddot{\delta}$  is the second derivative with respect to the time-like variable  $\tau$ .

$\tau$  is defined as  $\tau = \ln(t_e/t)$  where  $t$  is the time and  $t_e$  is the last time considered in this paper, close to equality. More specifically we have considered  $R_e = 10^{-5}$ , or  $t_e = 3.66 \times 10^9$  s, before the acoustic epoch.

$\nabla'$  is the Laplacian operator, when the spatial coordinates are  $x'_i$  instead of  $x_i$ , the usual comoving coordinates.

$x'_i$  is defined as  $x'_i = (K/R_e)x_i$ , where  $K$  is the constant in the expansion law  $R^2 = Kt$ . The value of  $K$  is  $2.73 \times 10^{-20} \text{s}^{-1}$  and therefore  $x'_i = 2.73 \times 10^{-15}x_i$ , where  $x_i$  are measured in seconds. The relation between  $x'_i$  and  $d$ , the length measured in present-day-Mpc is  $x'_i = 0.28(d/\text{Mpc})$ .

$X$  characterizes the magnetic energy density and is defined as

$$X = \frac{B_0^2}{24\pi p_0}$$

$B_0$  would be the present magnetic field if no source and no loss other than expansion had taken place after the time period considered here. Because the post-recombination epoch is probably very complicated, concerning the evolution of magnetic fields,  $B$  has in practice no relation with present magnetic

fields.  $\mathbf{B}_0$  is exactly defined as  $\mathbf{B}_0 = \mathbf{B}R^2$ . We measure magnetic field strengths in  $\text{s}^{-1}$ , with the equivalence being 1 Gauss  $= 8.61 \times 10^{-15} \text{ s}^{-1}$ .

$p_0$  is the relativistic particle hydrostatic pressure at present. It is defined as  $p_0 = pR^4$  and we have chosen the value  $p_0 = 8.84 \times 10^{-42} \text{ s}^{-2}$ .

$m$  also characterizes the magnetic field configuration

$$m = -\frac{1}{2}\nabla' \cdot \left( \frac{2}{3}\mathbf{n} - \nabla' X \right)$$

where

$$\mathbf{n} = -\frac{\mathbf{B}_0 \cdot \nabla \mathbf{B}_0}{4\pi p_0} + 3\nabla' X$$

To integrate our basic equation it is then necessary to specify the field. In this paper we analyze the influence of a magnetic tube flux, i.e.  $\mathbf{B}_0$  is given by

$$\mathbf{B}_0 = (0, 0, A)e^{-\frac{r^2}{2\sigma^2}} \quad (1)$$

where  $r$  and  $\sigma$  are measured with the same unit as  $x'_i$ . For instance  $\sigma = 1$  is equivalent to a comoving-length of 0.28 Mpc. For our purposes, the solution very much depends on the value of  $\sigma$  and we call it large scale if  $\sigma \gg 1$ , intermediate scale, if  $\sigma \approx 1$ , and small scale, if  $\sigma \ll 1$ .

In the particular case of a flux tube:

$$X = ae^{-\frac{r^2}{\sigma^2}}$$

where

$$a = \frac{A^2}{24\pi p_0}$$

and

$$m = \frac{2a}{\sigma^2} e^{-\frac{r^2}{\sigma^2}} \left( 2 - \frac{r^2}{\sigma^2} \right)$$

For integrating, it is better to define another time-like variable as

$$t' = e^{-\tau} = \frac{t}{t_e}$$

Using this dimensionless time the basic equation becomes:

$$\delta'' t'^2 + \delta' t' - \delta - X + \frac{1}{3} t' \nabla'^2 \delta + 2 t' m = 0 \quad (2)$$

where now  $\delta'$  and  $\delta''$  are first and second derivatives with respect to  $t'$ .

From now on we will write simply  $t$  instead of  $t'$  and  $x_i$  instead of  $x'_i$  without any risk of confusion.

## 2. The integration and boundary conditions

Eq. (2) is an elliptic linear second order differential equation with variable coefficients. From the physical point of view, it would be preferable to carry out the integration as an initial value problem, to start with an initial configuration and calculate the shape and density of the cloud at the final step, at  $t_e$ . However, elliptic differential equations cannot usually be integrated this way, and a unique solution does not exist. Our first attempts to treat the problem as an initial value problem were indeed very unstable, confirming this fact. Probably, this intrinsic instability of the equation is somewhat associated with a physical complexity. It was therefore necessary to look for a boundary value solution. In this case, a unique solution does exist, but as we must assume the final geometry of the cloud, the predictive possibilities are completely lost. Nevertheless, the evolution of the cloud can be followed by means of very stable methods and some combinations of free parameters and boundary conditions can be rejected if they provide physically implausible solutions.

We chose ‘‘Simultaneous Over-Relaxation’’ method (SOR) with Chebyshev acceleration (Press et al. 1989; Holt, 1984; Smith, 1985 and others).

The equation is written as

$$\begin{aligned} & \delta_{l+1,j} \left( l^2 + \frac{l}{2} \right) + \delta_{l-1,j} \left( l^2 - \frac{l}{2} \right) \\ & + \delta_{l,j+1} \left( \frac{l\Delta t}{3(\Delta x)^2} + \frac{l\Delta t}{6j(\Delta x)^2} \right) \\ & + \delta_{l,j-1} \left( \frac{l\Delta t}{3(\Delta x)^2} - \frac{l\Delta t}{6j(\Delta x)^2} \right) \\ & + \delta_{l,j} \left( -2l^2 - 1 - \frac{2l\Delta t}{3(\Delta x)^2} \right) \\ & - ae^{-j^2(\Delta x)^2/\sigma^2} - \frac{4al\Delta t}{\sigma^2} e^{-j^2(\Delta x)^2/\sigma^2} \left( \frac{j^2(\Delta x)^2}{\sigma^2} - 1 \right) = 0 \end{aligned}$$

or equivalently

$$a_{l,j}\delta_{l,j+1} + b_{l,j}\delta_{l,j-1} + c_{l,j}\delta_{l+1,j} + d_{l,j}\delta_{l-1,j} + e_{l,j}\delta_{l,j} = f_{l,j}$$

with obvious definitions of the coefficients  $a_{l,j}$ ,  $b_{l,j}$ ,  $c_{l,j}$ ,  $d_{l,j}$ ,  $e_{l,j}$  and  $f_{l,j}$ . Subindex  $l$  denotes time and subindex  $j$  the spatial variable  $r$ . The iterative method calculates a new  $\delta$  map from a previous step  $\delta$  map by

$$\delta_{l,j}^{new} = \delta_{l,j}^{old} - \omega \frac{\xi_{l,j}}{e_{l,j}}$$

where  $\xi$  is the residual calculated by

$$\begin{aligned} \xi_{l,j} = & a_{l,j}\delta_{l,j+1} + b_{l,j}\delta_{l,j-1} + c_{l,j}\delta_{l+1,j} \\ & + d_{l,j}\delta_{l-1,j} + e_{l,j}\delta_{l,j} - f_{l,j} \end{aligned} \quad (3)$$

and  $\omega$  is the relaxation parameter. When using Chebyshev acceleration,  $\omega$  is estimated at every iterative step. The network is divided into white and black points as in a chess-board. The value of  $\delta$  in white points is calculated from the previous step values of  $\delta$  in black points, and at the next step  $\delta$  in black points

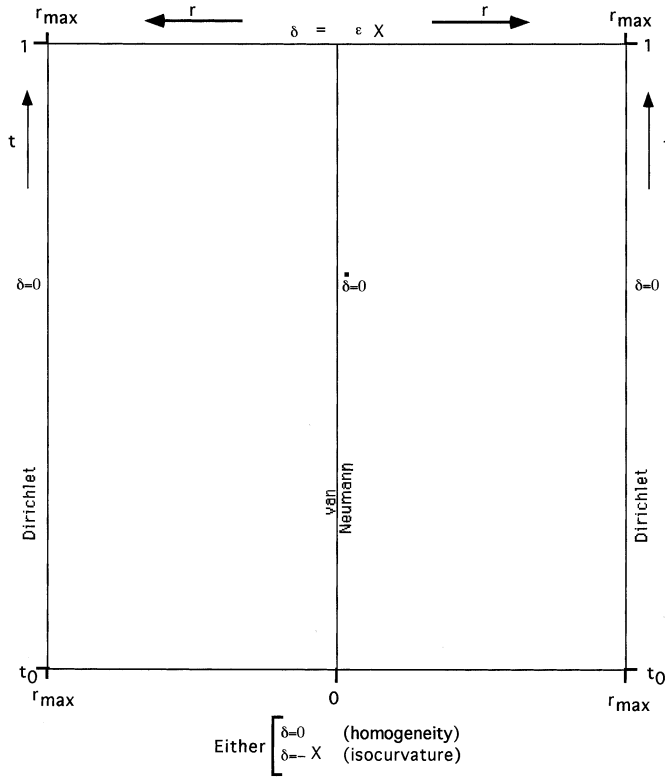


**Fig. 1.** Diagram of the boundary conditions

are calculated from  $\delta$  in white points. The relaxation parameter is calculated with the series

$$\begin{aligned} \omega^{(0)} &= 1 \\ \omega^{(1/2)} &= 1 / (1 - \rho_{Jacobi}^2 / 2) \\ &\dots \\ \omega^{(n+1/2)} &= 1 / (1 - \rho_{Jacobi}^2 \omega^{(n)} / 4) \\ &\dots \\ \omega^{(\infty)} &= \omega_{\text{optimus}} \end{aligned}$$

where

$$\rho_{Jacobi} = \frac{\cos \frac{\pi}{J} + \left(\frac{\Delta x}{\Delta t}\right)^2 \cos \frac{\pi}{L}}{1 + \left(\frac{\Delta x}{\Delta t}\right)^2}$$

if the size of the net is  $L \times J$ .

Convergence was usually obtained in less than 800 steps, and the solution is very stable.

We need to take boundary conditions in space and in time (see Fig. 1). Far from the flux tube (at about  $\pm 3\sigma$ ) we would have  $\delta = 0$ , for instance for  $r = 3\sigma$ . The other space-boundary could be either a van Neumann condition,  $\delta(r = 0) = 0$ , or again  $\delta(r = 3\sigma) = 0$  in the opposite direction. Because of the symmetry of the flux tube they must be equivalent, with the latter condition being more time and memory demanding. We have tried both and obtained the same result. This was one way to test the stability of the SOR.

With respect to the time-boundaries, we have at  $t = 0$  two possibilities. Either  $\delta(t = 0) = 0$ , which we call ‘‘homogeneity’’ or  $\delta(t = 0) = -X$ , which we call ‘‘isocurvature’’. In the first case, it is implicitly assumed that no inhomogeneities are initially present: these are subsequently produced by magnetic field structures. As the presence of magnetic fields introduces a metric perturbation, the isocurvature condition assumes that this energy density excess is initially compensated by an under-concentration of the dominant particles, so that the curvature is initially constant. We have numerically found that the two conditions produce different behaviours only in the very first time steps and that the evolution coincides through most of the period considered. This is discussed below. We have not begun at  $t = 0$  exactly but at  $t = 0.01$  (remembering that  $t$  varies between 0 and 1). On the one hand  $t = 0$  may introduce some instability, as discussed below, as foreseen in the theory. On the other hand  $t = 0$  is Big Bang time, which is beyond our scope.

At  $t = 1$ , we have adopted  $\delta(t = 1) = \epsilon X$ , i.e. with  $\delta(r)$  being a gaussian. The parameter  $\epsilon$  was adopted such that  $\delta(t = 1, r = 0)$  was  $10^{-4}$ , because this would be a typical value of  $\delta$  at  $t_e$ , in order to reproduce the present inhomogeneity field.

Results for low and intermediate scales were numerically found by the above described procedure. For the larger scales, it is shown later that the solution can be theoretically found.

### 3. Small and intermediate flux tube thickness

We have two basic parameters:  $\sigma$ , which determines the length-scale of the inhomogeneity, and  $a$ , which determines the magnetic field strength. After some initial trial calculations we decided to adopt  $a$  in the range  $10^{-5}$  to  $10^{-4}$ . A value much lower than this makes the problem a classical one in the absence of magnetic fields. A higher value produced unrealistic profiles with a large maximum at intermediate times: terms containing  $a$  were then of a larger order of magnitude and produced a large growth only restricted by our boundary conditions at  $t = t_e$ . Indeed, this leads us to an important conclusion: if  $a = 1$ , we have equipartition of magnetic field and radiative energy densities. This corresponds to an equivalent-to-present field strength of  $3 \mu G$ . Thus  $a = 10^{-5}$  would correspond to a present field strength of  $10^{-8} G$ . Fields as low as equivalent-to-present  $10^{-8} G$  are able to affect inhomogeneities in the time interval considered. If they are now measured to be higher than this, some amplification or dynamo mechanism must have taken place after recombination. Magnetic fields which are able to affect the small and intermediate scale inhomogeneities are also of the order of  $10^{-8} G$  (equivalent present values).

In Figs. 2 and 3, we plot our results for small scale flux tubes, with  $\sigma = 0.3$ . Fig. 2 shows the time evolution of the maximum perturbation at the flux tube axis for  $a = 10^{-5}$ , taking two different initial boundary conditions: isocurvature and inhomogeneity. We see that both initial conditions give the same results except for very early times. Fig. 3 shows the time evolution of the inhomogeneity profile. It remains essentially gaussian throughout the whole time period, increasing more rapidly in the recent half time period.

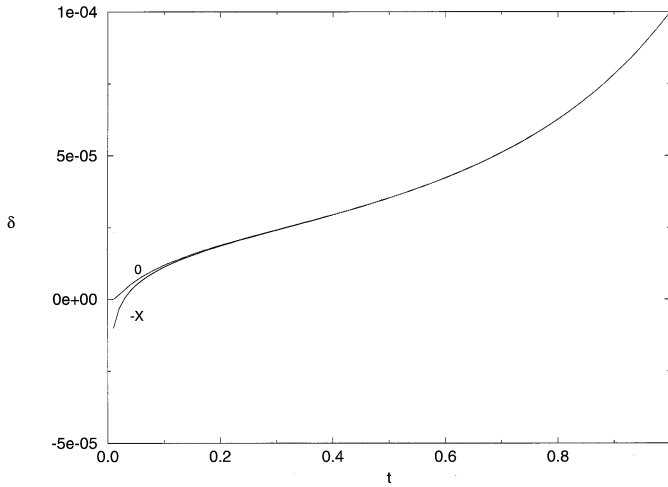


**Fig. 2.** Time evolution of the value of  $\delta$  at the centre of the filament, for  $\sigma = 0.3$  and  $a = 10^{-5}$ . Curve 0 for  $\delta(t_0) = 0$ . Curve -X for  $\delta(t_0) = -X$

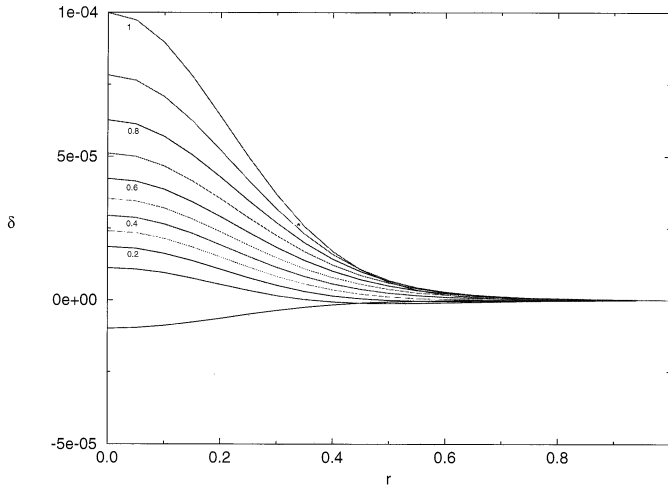


**Fig. 3.** Time evolution of the filamentary inhomogeneity profile for  $\sigma = 0.3$  and  $a = 10^{-5}$  for the boundary condition  $\delta(t_0) = -X$ . The parameter characterizing the different curves is a time parameter

In Figs. 4, 5, 6, we plot the results obtained for intermediate scale flux tubes, with  $\sigma = 1$ . Fig. 4 shows the time evolution of the maximum perturbation for  $a = 10^{-4}$ ,  $a = 10^{-5}$  and for both isocurvature ( $\delta(t_0) = -X$ ) and homogeneity ( $\delta(t_0) = 0$ ) initial conditions. The first one provides curves without a short initial decrease, which does not seem to be very realistic. For small magnetic fields we see again that the growth is faster in the last part of the time considered. For large magnetic fields the situation is more or less reversed. Fig. 5 shows the time evolution of the inhomogeneity profile, for moderate magnetic field strengths,  $a = 10^{-5}$ , and Fig. 6 for higher strengths. The latter shows significant departures from the gaussian profiles.

#### 4. Large scale flux tubes

In our basic Eq. (2) the last two terms have orders of magnitude of  $\delta/\sigma^2$  and  $a/\sigma^2$ , respectively. They can therefore be ignored

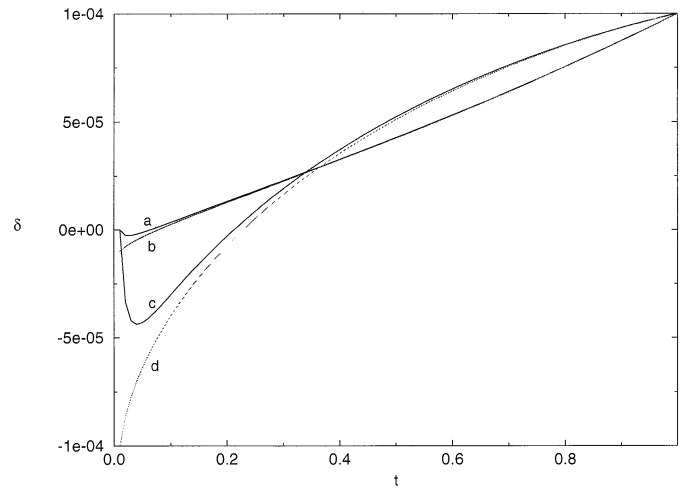


**Fig. 4.** Time evolution of the value of  $\delta$  at the centre of the filament, for  $\sigma = 1$ . Curve a:  $a = 10^{-5}$ ,  $\delta(t_0) = 0$ ; curve b:  $a = 10^{-5}$ ,  $\delta(t_0) = -X$ ; curve c:  $a = 10^{-4}$ ,  $\delta(t_0) = 0$ ; curve d:  $a = 10^{-4}$ ,  $\delta(t_0) = -X$

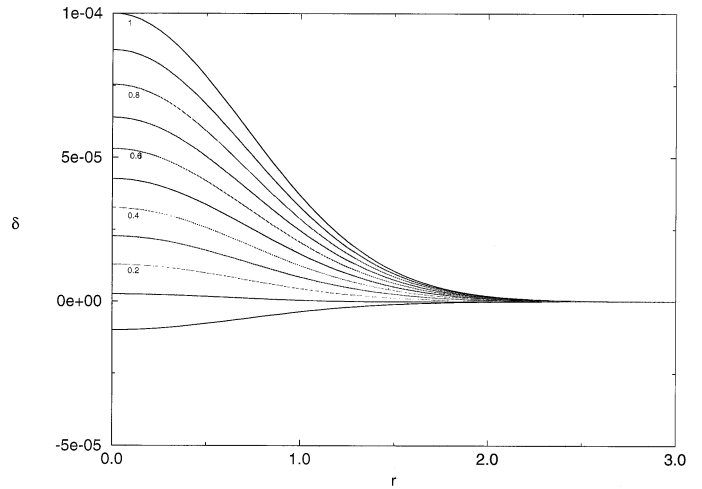


**Fig. 5.** Time evolution of the filamentary inhomogeneity profile for  $\sigma = 1$  and  $a = 10^{-5}$  for the boundary condition  $\delta(t_0) = -X$ . The parameter characterizing the different curves is a time parameter

when  $\sigma$  is very large. This fact is important for two reasons. From the integration point of view, if the laplacian term is negligible, the equation is no longer elliptic. It can be treated analytically and what is most noticeable is that it can be integrated as an initial-value problem, thus restoring the prediction ability of the equation. We do not need to assume the shape and magnitude of the inhomogeneity before the acoustic regime period. The other reason is that  $\sigma \gg 1$  probably represents a more interesting case as dissipative effects may wipe out small scale inhomogeneities after the time epoch considered in this paper.

The analytical solution now becomes

$$\delta = -X + c_1 t + \frac{c_2}{t}$$

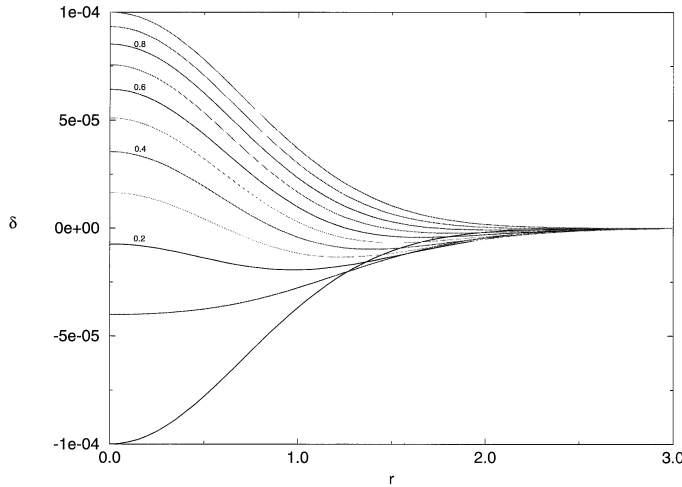


**Fig. 6.** Time evolution of the filamentary inhomogeneity profile for  $\sigma = 1$  and  $a = 10^{-4}$  for the boundary condition  $\delta(t_0) = -X$ . The parameter characterizing the different curves is a time parameter

where  $c_1$  and  $c_2$  are integration constants, which may be determined with the boundary conditions. We have several possibilities which should be discussed.

Suppose first that we are considering the time interval  $[0,1]$ . For  $t = 0$ , we have  $\delta = \infty$  unless  $c_2 = 0$ . But then  $\delta(t=0) = -X$ . Then only isocurvature would be a valid initial condition, and  $\delta = -X + c_1 t$ . However, we must avoid  $t = 0$  (Big-Bang) and begin with  $t = t_0$ , very small but non-vanishing. Also, in our numerical outputs we have carried out the integration since  $t = t_0 > 0$ . We have four options to determine  $c_1$  and  $c_2$ :

1) Boundary value and homogeneity. We assume  $\delta(t_0) = 0$  and  $\delta(t=1) = \epsilon X$ . The solution is then

$$\delta = -X + X(1 + \epsilon)t + \frac{X t_0}{t}$$

As  $t_0$  is low, this basically represents a linear growth.

2) Boundary value and isocurvature. We assume  $\delta(t_0) = -X$ ,  $\delta(1) = \epsilon X$

$$\delta = -X + X(1 + \epsilon)t + \frac{X(1 + \epsilon)t_0^2}{t}$$

where the last term is negligible. We again obtain a quasi-linear growth. As it was also numerically obtained, the conditions of homogeneity and isocurvature provide the same results, except in the beginning.

3) Initial value and homogeneity. We assume  $\dot{\delta}(t_0) = 0$  and obtain

$$\delta = -X + \frac{1}{2} \frac{X}{t_0} t + \frac{1}{2} X \frac{t_0}{t}$$

which also represents a nearly linear growth, but now the rate of growth  $X/2t_0$  is larger than the  $X(1 + \epsilon)$  in the two previous cases. In the end, we obtain  $\delta(1) = X \left(-1 + \frac{1}{t_0}\right) \approx X/t_0$ , i.e. the inhomogeneity grows  $1/t_0$ -fold, where  $t_0$  could be considered the magnetogenesis time, even if we adopted in the nu-

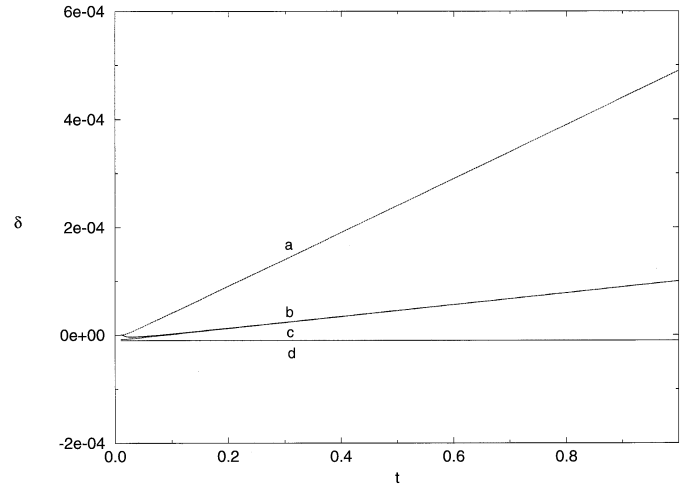


**Fig. 7.** Time evolution of the value of  $\delta$  at the centre of the filament, for  $\sigma \gg 1$  calculated with  $\epsilon = 10$ ,  $t_0 = 0.01$  and  $X_{max} = 10^{-5}$ . Curve a: Boundary value and homogeneity; Curve b: Boundary value and isocurvature; Curve c: Initial value and homogeneity; Curve d: Initial value and isocurvature. Curves b and c coincide except for small values of  $t$ , where curve b gives slightly higher values

merical integration in the previous section  $t_0 = 0.01$ . This third possibility has the best prediction ability.

4) Initial value and isocurvature. We assume  $\delta(t_0) = -X$  and  $\dot{\delta}(t_0) = 0$ . In this case, we obtain  $c_1 = c_2 = 0$  and therefore

$$\delta = -X$$

is a constant. No evolution is to be expected.

With the exception of the fourth, these possibilities all, basically, lead to the result already obtained for small scale flux tubes: the growth is more or less linear. The growth is plotted in Fig. 7 for the four possibilities mentioned above.

There is another analytical integration in another approach. Suppose that  $\sigma \gg 1$  and that  $a \gg \delta$ , so that only the laplacian term is negligible. The analytical solution becomes

$$\delta = (\ln t) t \frac{2a}{\sigma^2} e^{-\frac{r^2}{\sigma^2}} \left( \frac{r^2}{\sigma^2} - 2 \right)$$

but this solution does not represent a realistic case:  $\delta$  has a maximum at  $t = e^{-1}$ , vanishes at  $t = 1$ , and what is more important,  $\delta$  increases until it reaches values comparable to  $a$ , in contradiction with the initial assumption.

## 5. Conclusions

Primordial magnetic flux tubes are able to produce filamentary inhomogeneities of density which grow more or less linearly throughout the epoch considered in this paper. This epoch has been restricted from annihilation to just before the acoustic epoch, from  $z \approx 10^8$  to  $\approx 10^5$ , although the calculations may account for the evolution in epochs earlier than this time interval.

We have restricted ourselves to a particular case: that of a flux tube, or more specifically to the field configuration given by

Eq. (1). This choice was in part due to the frequent observation of flux tubes in other cosmic ionized systems and to the fact that they are suggested by the material filaments often observed in the large scale structure. It is also a very simple symmetric structure defined with only one coordinate. However this particular choice restricts the generality of our results and other field configurations are possible.

However, flux tubes, or at least structures as defined by Eq. (1), constitute a rather general case if we consider a universe with no mean magnetic field and in which the fluctuating field is made up of characteristic cells with a coherent internal field orientation, but having no “a priori” relation with the orientation of the field in adjacent cells. Suppose a coherence cell in which the field can be represented by  $(0,0,B_z)$ , with  $z$  clearly being the direction of the field within the cell. We look for a function  $B_z(x)$ , i.e. when we leave the cell following a perpendicular direction to the field in the cell. Before encountering another coherence cell,  $B_z(x)$  would vanish. In the opposite direction ( $-x$ ) we would have the same function. At the centre, we would have a maximum of  $B_z$ , with  $(\partial B_z/\partial x)_{x=0} = 0$ , avoiding a discontinuity in the second derivative. If we adopt axisymmetry, we conclude that  $B_z(r)$  can reasonably be assumed to be a Gaussian, as specified by our Eq. (1). It is true that flux tubes are long structures and the above argument does not consider the length of the structure defined by (1). Along  $z$ , the field can be independent of  $z$  and therefore represented by  $(0,0,B_z(r))$  within a  $z$ -length, which is considered long in this paper, but with an unimportant and unspecified value. Therefore, even if we consider a particular magnetic field configuration as our basic structure, our results remain rather general.

After the epoch considered in this paper, other effects, such as damping of small diameter filamentary structures prior to recombination, non-linear growth after recombination and mechanisms amplifying magnetic fields in recent pregalactic and galactic epochs, will complicate this simple picture, but this is beyond our objectives.

Our work is restricted to an unobservable epoch, which means that our results cannot strictly be compared with observations. Its objective is to provide initial conditions for other models devoted to more recent epochs, the whole history of cosmological magnetism being a huge task, which cannot be undertaken by a single model. Nevertheless, it is unlikely that large filamentary structures have disappeared in more recent epochs, so that our results may provide an explanation for presently observed large scale structures. The implications of this model in their interpretation are in part, considered in Paper III. It is really to be expected that large structures remain unaffected by complex processes after equality. This is justified as follows:

Damping of cosmic magnetic fields has been considered by Jedamzik, Katalinic and Olinto (1997) introducing viscosity, bulk viscosity and heat conduction. After neutrino decoupling the main damping mechanism is photon diffusion, which only affects structures up to the Silk mass, about  $10^{13} M_\odot$ .

When considering the growth of unmagnetized structures, it is assumed that non-linear effects are important only at smaller scales, up to  $\sim 10$  Mpc, and this limit probably remains valid

when magnetic fields are taken into account. In practice, this limit corresponds to the scale at which the rms galaxy fluctuations are unity, and is therefore independent of the involved forces. This issue has been considered by Kim, Olinto and Rosner (1996).

Finally, we must take into account specific mechanisms of magnetic field creation and amplification in recent times. A large variety have been proposed (Zwibel, 1988; Pudritz and Silk, 1989; Harrison, 1973; Tajima et al., 1992; Lech and Chiba, 1995, and others); See also the reviews by Rees (1987) and Kronberg (1994). The important fact is that these mechanisms induce small scale magnetic fields, smaller than a few Mpc. As far as we are aware, no mechanism for producing magnetic fields at scales larger than a few Mpc have been proposed for post-Recombination mechanisms.

After Equality, some mechanisms erase pre-existing magnetic fields, and others amplify them in a complicated way, thus modifying the pre-Equality magnetic fields considered in this paper, although these mechanisms only affect the small scale structures. The evolution of large scale structures could be described by the formulae in Appendix B into Paper I, i.e., the structures are maintained, simply growing with the expansion. Our model therefore, constitutes a tool to interpret present large scale structures.

It is a well established observational fact that the large-scale structure of the Universe is very rich in filaments (Gregory and Thomson, 1978; Oort, 1983; de Lapparent et al. 1986 and others. See for instance the review by Einasto, 1992) being more abundant than two-dimensional sheets (Shaty, Sahni and Einasto, 1992). They can play an important role in the formation of clusters (West, Jones and Forman, 1995).

The existence of large-scale filaments is currently accounted for by other hypotheses, but it is here suggested that primordial magnetic flux tubes constitute an additional alternative, or at least, a mechanism reinforcing other gravitational effects. Filaments are associated with magnetic fields in many astrophysical systems, such as the Sun and the interstellar medium, and we now see that this association can be extended to large-scale filamentary structures in the Universe.

The best studied large-scale filamentary structure is the Coma-A1367 supercluster, which is itself elongate and extended towards the Hercules supercluster. Its diameter is about 10 Mpc, thus constituting a large scale inhomogeneity in the sense considered here (i.e.  $\gg 0.28$  Mpc;  $\gg 1$  in the units defined above). Its length can be very large (Batuski and Burns, 1985). The distribution of early type galaxies is particularly thick (Doi et al., 1995).

As observed random velocities of groups and clusters with respect to the filament structure are relatively small ( $\sim 100$  Km  $s^{-1}$ ; Tully, 1982) the observed distribution of galaxies reflects its distribution when the whole structure was formed. The evolution of the filament and of the network of filaments it belongs to, has evolved very little.

Rather interestingly, the magnetic field strength has been measured in this supercluster. In a region well outside the coma cluster in the direction toward A1367, Kim et al. (1989) ob-

served a bridge of synchrotron emission with the same direction, of about  $0.3\text{--}0.6 \mu\text{G}$ , a large value for an extragalactic region. In the Coma cluster core region it is even larger, of the order of  $1.7 \mu\text{G}$  (Kim et al. 1990). Radio observations of the Coma cluster and its vicinity at different frequencies have been reported by Kim et al (1994) and Kim (1994). It would be very interesting to determine whether the direction of the magnetic field coincides with the NE-SW direction, which is that of the huge filament. This coincidence would be in noticeable agreement with the model here suggested.

## References

- Batuski, D.J., Burns, J.O. 1985, ApJ, 299, 5  
Doi, M., Fukugita, M., Okamura, S., Turner, E.L. 1995, AJ, 109, 1490  
Einasto, J. 1992, "Large-scale structure of the Universe" in Observational and Physical Cosmology, ed. by F. Sanchez, M. Collados & R. Rebolo. Cambridge Univ. Press. Cambridge. P. 251.  
Garrido, J.L., Battaner, E., Sanchez-Saavedra, M.L., Florido, E. 1993, AA, 271, 84  
Gregory, A., Thomson, L.A. 1978, ApJ, 222, 411  
Harrison, E.R. 1973, MNRAS, 147, 279  
Hawley, D.L., Peebles, P.J.E. 1975, AJ, 80, 477  
Jedamzik, K., Katalinic, V., Olinto, A. 1997, Submitted to ApJ  
Kim, E., Olinto, A., Rosner, R. 1996, ApJ, 468, 28  
Kim, K.T. 1994, A&AS, 105, 403  
Kim, K.T., Kronberg, P.P., Dewdney, P.E., Landecker, T.L. 1990, ApJ, 355, 29  
Kim, K.T., Kronberg, P.P., Dewdney, P.E., Landecker, T.L. 1994, A&AS, 105, 385  
Kim, K.T., Kronberg, P.P., Giovannini, G., Venturi, T. 1989, Nature, 341, 720  
Kronberg, P.P., 1994, Reports on Progress in Physics, 57, 325  
de Lapparent, V., Guller, M.J., Huchra, J.P. 1986, ApJ, 302, L1  
Lech, H., Chiba, M. 1995, AA, 297, 305  
Oort, J.H. 1983, ARA&A, 21, 373  
Pudritz, R.E., Silk, J. 1989, ApJ, 342, 650  
Rees, M.J. 1987, Q.J.R. astr. Soc., 28, 197  
Sathy, A.B.S., Sahni, V., Shandarin, S.F. 1996, ApJ, 462, L5  
Tajima, T., Cable, S., Shibata, K., Kulsrud, R.M. 1992, ApJ, 390, 309  
Tully, R.B. 1982, ApJ, 257, 389  
West, M., Jones, C., Forman, W. 1995, ApJ, 451, L5  
Zweibel, E.G. 1988, ApJ, 329, L1